Article

Structural and Functional Analysis of SHP Promoter and Its Transcriptional Response to FXR in Zn-Induced Changes to Lipid Metabolism

Han Gao [1,†], Xing Fan [1,†], Qi-Chun Wu [1,†], Chuan Chen [1], Fei Xiao [1] and Kun Wu [1,2,*]

[1] College of Marine Sciences, South China Agricultural University, Guangzhou 510642, China; 19865040582@163.com (H.G.); fx13006878436@163.com (X.F.); h15859679623@163.com (Q.-C.W.); cc18190392889@163.com (C.C.); xf15521300836@163.com (F.X.)

[2] University Joint Laboratory of Guangdong Province, Hong Kong and Macao Region on Marine Bioresource Conservation and Exploitation, Guangzhou 510642, China

* Correspondence: wk@scau.edu.cn or wk901012@126.com

† These authors contributed equally to the work.

Abstract: Zinc alleviates hepatic lipid deposition, but the transcriptional regulatory mechanisms are still unclear. In this study, we characterized the promoter of an SHP (short heterodimer partner) in a teleost *Pelteobagrus fulvidraco*. The binding sites of an FXR (farnesoid X receptor) were predicted by the SHP promoter, indicating that the FXR mediated its transcriptional activity. The site mutagenesis and the EMSA (electrophoretic mobility shift assay) found that the $-375/-384$ bp FXR site on the SHP promoter was the functional binding locus responsible for the Zn-induced transcriptional activation. A further study of yellow catfish hepatocytes suggested that the activation of the FXR/SHP is responsible for the effect of Zn on the decreasing lipid content. Thus, this study provides direct evidence of the interaction between the FXR and SHP promoter in fish, and accordingly elucidates the potential transcriptional mechanism by which Zn reduces hepatic lipid accumulation.

Keywords: SHP; promoter analysis; lipid metabolism; zinc; fish

1. Introduction

Zinc (Zn) is an essential micronutrient for many important biochemical processes in vertebrates. In recent decades, extensive studies have focused on its essential roles or toxic effects on growth, survival, reproduction, histological changes, redox response and immunity [1–3]. Recently, there has been a growing body of studies that recognizes the importance of Zn on metabolic processes, especially on the lipid metabolism. Zn deficiency is associated with a higher risk of fatty liver disease and an impaired lipid profile [4]. Clinical trials in humans and animals demonstrate that Zn plays a pivotal protective role in regulating the lipid profile and metabolism [4–6]. In fish, Zn accumulation can reduce lipid deposition. For example, Wu et al. [7] found that waterborne Zn exposure for 56 days reduced hepatic lipid deposition in *S. hasta*. Both chronic waterborne and dietary Zn reduced the tissue lipid content of yellow catfish by inhibiting lipogenesis and stimulating lipolysis [8,9]. Hence, Zn is considered to have the potential to prevent excessive lipid accumulation and maintain lipid homeostasis. However, the underlying molecular mechanisms have not been fully characterized in fish.

Lipids are essential nutrients and play important roles in metabolic processes. In fish, the failure to maintain lipid homeostasis impedes a wide range of physiological processes [10]. In general, lipid homeostasis is characterized by the balance between lipogenesis and lipolysis, which are regulated by transcriptional factors and crucial genes. The farnesoid X receptor (FXR) and short heterodimer partner (SHP/NR0B2) are important nuclear receptor and transcription factors controlling lipid metabolism [11,12]. The SHP

plays important roles in regulating the expression of genes, with roles in bile acid transport, lipid metabolism and gluconeogenesis [13]. In eukaryotic organisms, promoters have many cis-acting elements and can be bound by transcriptional factors, which activate the transcription initiation, thereby regulating gene expression. Studies in mice suggest that the FXR is an upstream regulator of the SHP and targets the SHP promoter [13]. In a teleost, extraordinarily little is currently known about the interaction between the FXR and SHP. Our recent study suggested that the FXR/SHP pathway may constitute a crucial link between the tissue Zn content and the prevention of lipid accumulation [12,14]. Thus, it is crucial to analyze the structure and function of the SHP promoter, which may decipher the mechanism of Zn-regulating target genes relevant to lipid metabolism and lead to new treatments for fatty liver diseases.

The yellow catfish (*Pelteobagrus fulvidraco*) is an omnivorous freshwater fish commonly farmed in China and other countries for the excellent fillets and high market value. Under intensive aquaculture, this fish species frequently exhibits excessive hepatic lipid deposition and severe fatty liver syndrome, which have adverse effects on its health [12]. Thus, it is especially important and meaningful to research ways to reduce lipid deposition and the underlying molecular mechanisms. Given the potential role of Zn on the FXR/SHP pathway and the role of the pathway on lipid deposition [12,14], we hypothesize that the SHP acts as a mediator in the Zn-induced effects on lipid metabolism. In the present study, we identified the SHP promoter region of yellow catfish and investigated its functional bind with the FXR under the Zn signal. Our study offers innovative insights into the mechanism of Zn-regulating SHP transcriptional activity and lipid deposition, which are important for the evaluation of Zn nutrition and the regulatory effects on lipid metabolism in vertebrates.

2. Results

2.1. Cloning and Sequence Analysis of the SHP Promoter

In the present study, the 1790 bp SHP promoter of a yellow catfish was successfully cloned (Figure 1A). On the SHP promoter region, we predicted several core promoter elements, such as a TATA-box (TBP) located from −81 bp to −90 bp and a CCAAT-box (NF-Y) located at −101 bp to −110 bp (Figure 1B). We also predicted a cluster of binding sites of several transcription factors on the SHP promoter, including the FXR, EERγ (estrogen receptor-related receptor γ), Sp1 (GC-box), STAT3 (signal transducer and activator of transcription 2), PPARα/RXR (peroxisome proliferator-activated receptor α/retinoid X receptor) and KLF4 (Kruppel-like factor 4) (Figure 1B).
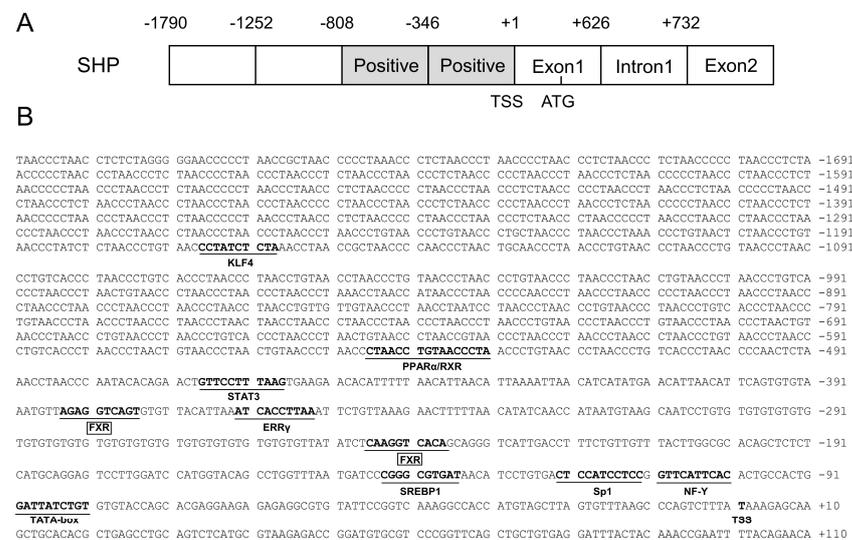

Figure 1. (**A**) The schematic diagram of SHP gene structure. The first nucleotide of 5′ cDNA of SHP was designated as +1. Positive: the region that positively regulated the promoter activity. TSS: transcription

start site. ATG: translation initiation site. (**B**) Nucleotide sequence of yellow catfish SHP promoter. Numbers are relative to the transcription start site (+1). The putative transcription factor binding sites are underlined. The highlighted sequences show putative transcription factor binding sites of FXR.

2.2. The 5′-Deletion Assay of the SHP Promoter

In the present study, we randomly generated plasmids of a distinct size and selected four appropriate plasmids to perform the 5′-deletion assay. The sequence deletion from −1790 bp to −808 bp showed no significant effects on the luciferase activity, but the deletion from −808 to −346 bp reduced the luciferase activity significantly (Figure 2).
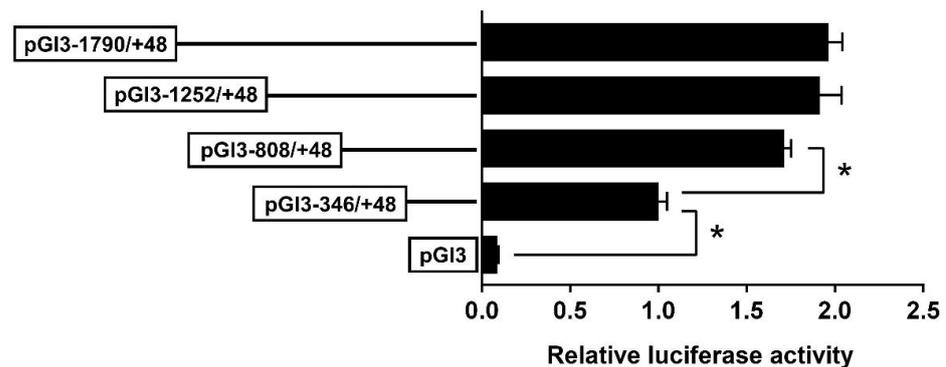

Figure 2. The 5′ unidirectional deletion assays of the SHP promoter region of yellow catfish. Values mean the ratio of activities of firefly to Renilla luciferase normalized to the control plasmid. Results are shown as mean ± SEM (*n* = 3). Asterisk (*) means significant differences between the two groups ($p < 0.05$).

To investigate the response of the promoter to Zn, HepG2 cells were incubated with 50 μM Zn^{2+} for 48 h and then the 5′ deletion assay was performed. Compared to the control, Zn significantly increased the luciferase activities of pGl3-1790/+39, pGl3-1252/+39 and pGl3-808/+39, but had no effect on pGl3-346/+39. In the Zn-treated group, the sequence deletion between −1790 bp and −808 bp of the SHP promoter showed no significant influences on luciferase activity; however, further deletion to −346 bp down-regulated the luciferase activity (Figure 3).
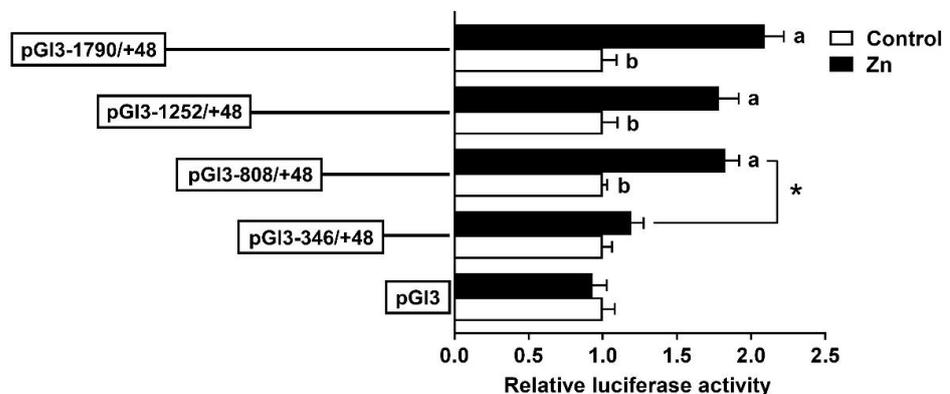

Figure 3. The 5′ unidirectional deletion assays for promoter regions of SHP after 50 μM Zn treatment. Values show the ratio of activities of firefly to Renilla luciferase normalized to the control. Results are presented as mean ± SEM (*n* = 3). Asterisk (*) indicates significant differences between different 5′ unidirectional deletion plasmids under the same treatment ($p < 0.05$). Different letters indicate significant differences between the different treatments in the same plasmid ($p < 0.05$).

2.3. Site Mutation Analysis of FXR Binding Sites on the SHP Promoter

Based on the results of the 5′-deletion assay, we performed the site mutation using the pGl3-1790/+39 plasmid. The mutation of the −267/−276 FXR binding site (Mut-FXR-2) did not change the Zn-induced elevation of luciferase activity, suggesting that this site played no role in the SHP transcriptional response to Zn. In contrast, the mutation of the −375/−384 FXR binding site (Mut-FXR-1) decreased the Zn-induced luciferase activity significantly. Similarly, the co-mutation of the −267/−276 and −375/−384 binding sites (Mut-FXR-1 and 2) also down-regulated the Zn-induced increase in luciferase activity, indicating that the −375/−384 FXR binding site positively mediated the activity of the SHP promoter (Figure 4).
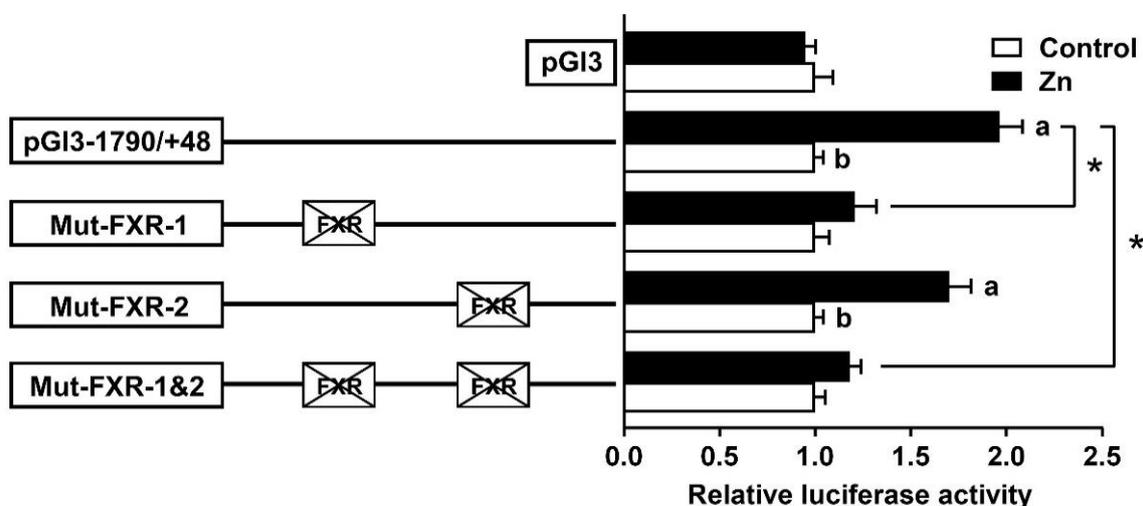

Figure 4. Assays of predicted FXR binding sites after site-directed mutagenesis. Values mean the ratio of activities of firefly to Renilla luciferase normalized to the control. Results are presented as mean ± SEM (*n* = 3). Asterisk (*) indicates significant differences between the different mutation plasmids under the same treatment (*p* < 0.05). Different letters indicate significant differences between different treatments in the same plasmid (*p* < 0.05).

2.4. FXR Bind with the SHP Promoter

Based on the mutation assays and transcriptional analysis, we speculated that the FXR could bind with the sequence from −375 to 384 bp of the SHP promoter, thereby activating the transcription of the SHP and its downstream genes. Thus, we further used the EMSA (electrophoretic mobility shift assay) to detect the physical interaction between the transcription factor FXR and the specific binding site on the SHP promoter. As shown in Figure 5, when the FXR binding sequence was used as the probe, the 100-fold unlabeled binding sites (between −375 and −384 bp of the SHP promoter) competed for binding. In contrast, the 100-fold unlabeled Mut-FXR1 binding sites declined this competition significantly, indicating that this region could be bound by the FXR. Meanwhile, the increased brightness of bands under the Zn treatment reflected that Zn promoted the binding process between the FXR and this binding position on the SHP promoter.
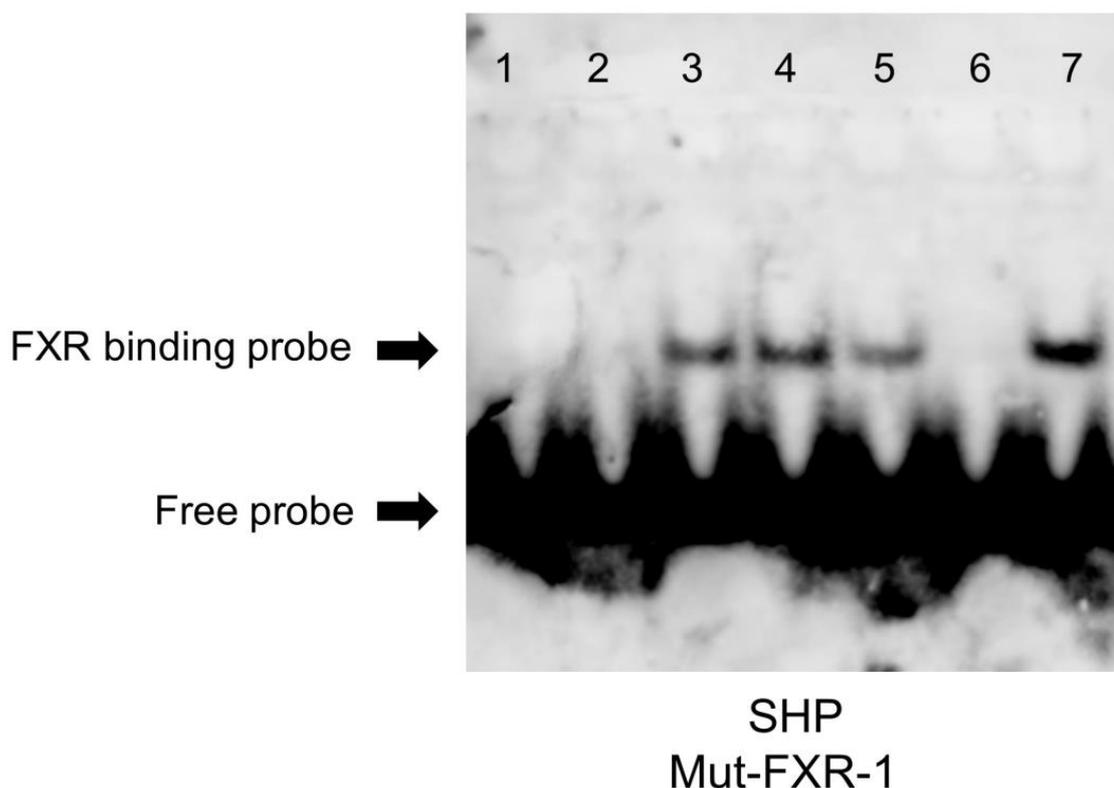
Figure 5. EMSA of predicted FXR binding sequence on yellow catfish SHP promoter (between −375 bp and −384 bp). NP, nuclear protein. The numbers 1–7 represent the 7 different lanes.

2.5. Effect of Zn on Lipid Metabolism of Yellow Catfish Hepatocytes

Compared with the control, 50 μM Zn significantly increased the intracellular Zn concentration (Figure 6A), but decreased the contents of lipid droplets (Figure 6B) and TG (Figure 6C). We further detected mRNA levels of the FXR/SHP pathway and its downstream genes. Zn activated the FXR/SHP pathway because of the increased expression of the *fxr* and *shp* (Figure 6D). For genes involved in lipogenesis, Zn down-regulated the expression of *accα* and *fas*, but had no effect on *g6pd* and *6pgd*. Additionally, the expression of *cpt1α*, a key gene in fatty acid β-oxidation, was increased by Zn incubation. In general, Zn promoted the lipolytic processes but suppressed the lipogenic processes in the yellow catfish hepatocytes.
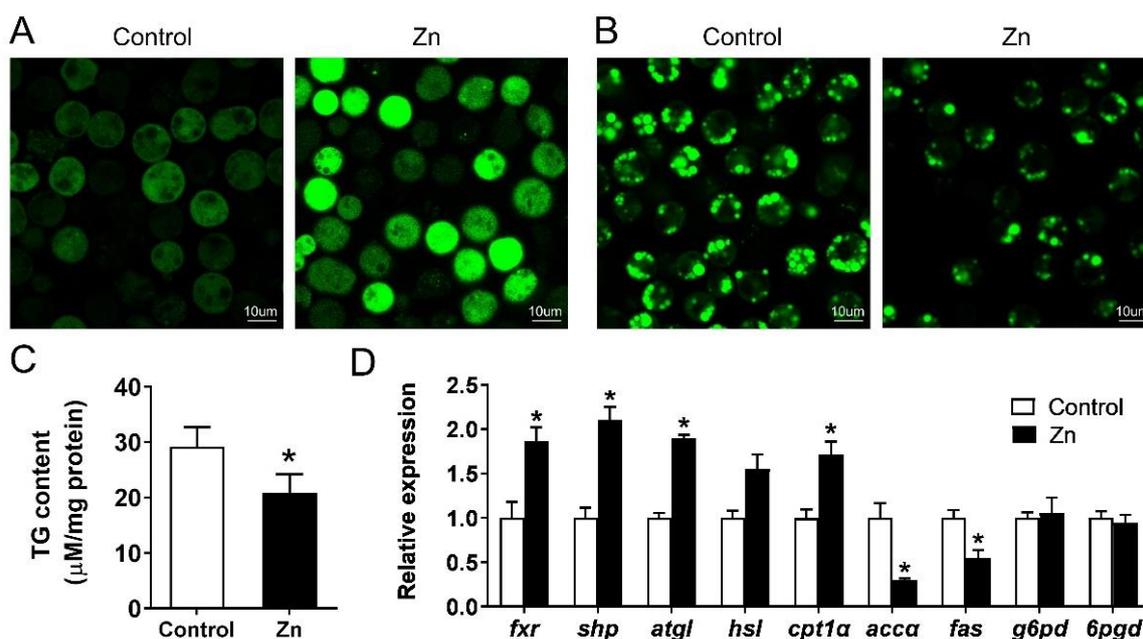
Figure 6. Effect of Zn incubation on cellular Zn concentration. (**A**): lipid droplet contents; (**B**): TG accumulation; (**C**): mRNA levels involved in lipid metabolism; (**D**): in hepatocytes of yellow catfish at 48 h. Results are presented as mean $\pm$ SEM (n = 3). Asterisk (*) indicates significant differences in different treatments ($p < 0.05$).

3. Discussion

Previous studies indicated that the FXR and SHP play important roles in regulating lipid-metabolism-related genes in yellow catfish [12,14], but direct evidence has not been explored. This study, for the first time, cloned and characterized the structure and function of the SHP promoter region from a yellow catfish and investigated its transcriptional response to the FXR in Zn-induced changes in lipid metabolism.

The first step for exploring the mechanism of transcriptional initiation is the identification of the core promoter, which is located most proximal to the start codon and contains the RNA polymerase binding sites [15]. In this study, one TATA-box, one CAAT-box (NF-Y) and one GC-box (Sp1) binding sites were found in the core SHP promoter region (Figure 1). The TATA-box and CAAT-box were commonly found at upstream sites close to the TSS and helped to dock the RNA polymerase transcriptional complex [16]. In fact, only approximately 5%–7% of the eukaryotic promoters had a TATA-box [15], and TATA-less promoters usually possessed Sp1 binding sites, which drive the basal transcription function [17]. In mammals, different splicing yields two SHP promoters and both of the two isoforms contain a TATA-box, CAAT-box and GC-box [18,19]. The similar arrangement of core promoter elements between the yellow catfish and mammals indicate that their SHP promoters have similar transcriptional initiation modes and conserved functions.

The identification of transcription factor binding sites (TFBSs) helps to decipher the regulatory mechanisms of genes. The present study showed that the luciferase activities of the SHP promoter underwent almost no changes when the sequence increased from -1790 bp to -808 bp, which may be attributable to the lack of key binding sites in this region. In contrast, the luciferase activity decreased when the sequence from -808 to -346 bp was deleted (Figure 2). A further investigation found that this region contained a cluster of TFBSs, such as the FXR, STAT3, ERRγ, PPARα/RXR and SREBP1 (Figure 1B). In mammals, these transcription factors have been identified to activate the SHP promoter and regulate SHP expression [13,20,21]. Thus, the putative transcription factors in the region from -808 to -346 bp are likely to be positive regulators of the SHP gene (Figure 1A). Notably, most of these transcription factors engage in lipid metabolism and obesity [22], suggesting that the SHP probably plays a role in the regulation of lipid metabolism. Indeed, multiple lines

of evidence demonstrate that the SHP regulates several metabolic pathways by responding to other nuclear receptors and transcription factors [13]. Further, Zn incubation markedly increased the activity of the SHP promoter from −808 to −346 bp (Figure 3), indicating that Zn promotes SHP transcription, in agreement with a previous study in mouse and human cells [23]. Studies have suggested that Zn stimulates lipolysis and inhibits lipogenesis [7–9]. Our recent studies demonstrated the importance of the FXR/SHP pathway in regulating genes involved in lipid metabolism [12], especially under Zn action [14]. Considering that two putative FXR binding sites were positioned between −808 and −346 bp, this promoter sequence may be the pivotal region that responds to the zinc signal and regulates lipid metabolism in yellow catfish.

We next explored whether the FXR exerts regulatory action directly through these response elements. According to the putative results, two FXR binding sites were located on the region from −808 to −346 bp. However, a site mutation on the −375/−384 FXR binding site, but not on the −267/−276 binding site, reduced the Zn-induced increase in promoter activity (Figure 4). Information is extremely scarce about the direct interaction between the FXR and SHP in fish. In the present study, results of an EMSA further confirmed that the −375/−384 bp sequence was a functional binding site, and that Zn incubation promoted the FXR binding to this site because of the stronger band in the Zn-treated group (Figure 5). Similarly, Hoeke et al. [24] reported that the FXR regulated human SHP expression primarily via direct binding to key elements on the SHP promoter. The FXR is a ligand-modulated transcription factor and tightly controls bile acid synthesis and hepatic lipid metabolism through the induction of the SHP [25]. Therefore, the −375/−384 bp FXR site may play a vital role in responding to the Zn-induced up-regulation of SHP promoter activity.

Having determined the fact that the FXR stimulates SHP transcription by integrating with its promoter, we next explored their roles in the Zn-induced regulation of lipid metabolism using primary hepatocytes of yellow catfish. As shown in Figure 6, the increase in the intracellular Zn content reduced the deposition of lipid droplets and TG, like other studies [4,7–9]. Previous studies emphasize the importance of the FXR/SHP pathway in the regulation of lipid metabolism [12,14]. A high correlation between the FXR/SHP mRNA levels and the expressions of other genes involved in lipid metabolism was likewise observed in this study (Figure 6D). In general, the activation of the FXR/SHP pathway up-regulated the mRNA levels of lipolysis genes (*atgl* and *cpt1α*) and down-regulated the expression of lipogenesis genes (*accα* and *fas*), in agreement with the observations of lipid droplets and TG. Animal experiments showed that the SHP is an important target gene of the FXR in the regulation of lipid metabolism [26]. The SHP alleviates hepatic lipid deposition and obesity by acting as a transcriptional repressor of other lipogenic genes [13,27]. Considering the results of the site mutation assays and the EMSA, the FXR could directly bind with the SHP promoter, which could potentially mediate the regulation of lipid metabolism by Zn.

In conclusion, we identified and characterized the promoter region of the SHP gene from yellow catfish. In addition, we investigated the important roles of the FXR/SHP in Zn-induced changes in lipid metabolism. The present study provides the first direct evidence for the interaction between the FXR and SHP in fish, and accordingly elucidates the potential mechanism by which Zn reduces hepatic lipid accumulation.

4. Materials and Methods

4.1. Experimental Animals and Reagents

Yellow catfish were obtained from a local commercial farm (Guangzhou, China). HepG2 cell lines were obtained from the Cell Resource Center of our college. Dulbecco's Modified Eagle Medium (DMEM) and fetal bovine serum (FBS) were purchased from Gibco (Thermo Fisher Scientific, Waltham, MA, USA). The experiments complied with the ethical guidelines of South China Agricultural University (SCAU), Guangzhou, China, for the use of experimental animals and cells.

4.2. Promoter Cloning and Plasmid Construction

The hiTAIL-PCR (high-efficiency thermal asymmetric interlaced PCR) method [28] was used to clone the promoter sequences, and the protocols followed our previous studies [29,30]. The specific primers were listed in the Supplementary Table S1. The luciferase reporter constructs were produced via the purified PCR product and pGl3-Basic vectors (Promega, Madison, WI, USA), and the ClonExpress II One Step Cloning Kit (Vazyme, Piscataway, NJ, USA) was used to ligate the products. Based on the distance from the TSS (transcription start sites), we named the plasmids as pGl3-1790/+48 of SHP vector. Then, using the pGl3-1790/+48 vector as a template, we generated pGl3-346/+48, pGl3-808/+48, pGl3-1252/+48 vectors with the Erase-a-Base system (Promega, Madison, WI, USA). The primer sequences for plasmid construction are shown in Supplementary Table S2.

4.3. Sequence Analysis and Activities Assays of Luciferase

The transcription factor binding sites (TFBS) were predicted by the JASPAR database (http://jaspar.genereg.net/ (accessed on 10 December 2020)) and MatInspector (http://www.genomatix.de/ (accessed on 10 December 2020)). The reference binding site sequences are listed in the Supplementary Table S3.

Plasmid transfections and activity assays of luciferase followed our recent publications [29,30]. Briefly, HepG2 cells were cultured in DMEM medium (10% FBS) in an incubator with 5% CO_2 at 37 °C. Prior to the transient transfection, cells were seeded in a 24-well cell culture plate at a density of 1.2×10^5 and cultured for 24 h to reach 70%–80% convergence. Plasmids were transiently transfected into HepG2 using Lipofectamine 2000 (Invitrogen, Carlsbad, CA, USA). The reporter plasmids were co-transfected with 35 ng pRL-TK as control. After 4 h, DMEM (10% FBS) or DMEM (10% FBS) + 50 µM Zn were used to replace the transfection medium. After 24 h incubation, we used Dual-Luciferase Reporter Assay System to measure the relative luciferase activity according to the manufacture's manuals.

4.4. Site Mutation Assays of FXR Binding Sites on the SHP Promoter

Site mutation assays were performed to identify the FXR binding sites on the SHP promoter. The pGl3-1790/+48 vector was used as the template and the QuickChange II Site-Directed Mutagenesis Kit (Vazyme, Piscataway, NJ, USA) was used to conduct site-directed mutagenesis. The primers for mutagenesis are shown in Supplementary Table S4. The constructs were named Mut-FXR-1 and Mut-FXR-2. The pRL-TK and constructs were transfected into HepG2 according to the methods described in Section 4.3. After 24 h incubation, cells were harvested and the luciferase activities were detected.

4.5. Analysis of Functional Binding Sites of FXR on the SHP Promoter

An electrophoretic mobility shift assay (EMSA) was conducted to determine the functional binding site of FXR on the promoter region of SHP. Proteins for electrophoretic mobility shift assay (EMSA) were extracted from primary hepatocytes of yellow catfish. The EMSA protocol followed the instruction of the LightShift Chemiluminescent EMSA Kit (Invitrogen, Carlsbad, CA, USA) as in our previous studies [29,30]. Briefly, each oligonucleotide duplex of the FXR binding sites were incubated with 10 µg nuclear extracts. Before the biotin-labeled probe was added, each unlabeled probe was pre-incubated for 10 min. The biotin-labeled probe was added at room temperature and the reaction continued for 30 min. Then, they were detected via electrophoresis on 6% native polyacrylamide gels. This research performed competition analyses by using 100-fold unlabeled oligonucleotide duplex with or without the mutation. The oligonucleotide sequences of EMSA are shown in Supplementary Table S5.

4.6. Zn, LD and TG Contents in Hepatocytes and Gene Expression

We isolated hepatocytes from yellow catfish liver tissues according to our recent publications [12]. After 48 h incubation, intracellular Zn and LD were detected based on the protocols of our previous studies [12,31]. For detection of intracellular Zn^{2+} concentration, cells were incubated with 1 μM Newport Green DCF (Invitrogen, Carlsbad, CA, USA) for 30 min. For intracellular LD staining, cells were incubated with 5 mg/mL Bodipy (Invitrogen, Carlsbad, CA, USA) for 30 min. Fluorescence was imaged using laser scanning confocal microscopy (Leica, Wetzlar, Germany). We used the commercial assay kits (Nanjing Jian Cheng Bioengineering Institute, Nanjing, China) to analyze intracellular TG content. The mRNA levels of genes involved in lipid metabolism were examined by quantitative real-time PCR (Q-PCR). Primers are given in the Supplementary Table S6.

4.7. Statistical Analysis

SPSS 22.0 software (SPSS, Chicago, IL, USA) was used to conduct statistical analyses. Results are presented as mean ± standard errors of means (SEM). Before analysis, we used the Kolmogorov–Smirnov test to determine the normality of distribution of all data. The Student's *t*-test was used to compare the differences between wild types and treated group. Significant levels were set at $p < 0.05$.

Supplementary Materials: The following supporting information can be downloaded at: https://www.mdpi.com/article/10.3390/ijms23126523/s1.

Author Contributions: K.W. designed the experiment; H.G., X.F. and Q.-C.W. undertook the experiment and the sample analysis with the skilled help of C.C. and F.X.; H.G., X.F. and Q.-C.W. analyzed all the experimental data; H.G., X.F. and Q.-C.W. drafted the present paper; K.W. revised the papers. All authors have read and agreed to the published version of the manuscript.

Institutional Review Board Statement: Not applicable.

Informed Consent Statement: Not applicable.

Data Availability Statement: Not applicable.

Conflicts of Interest: The authors declare that they have no competing interests.

References

1. Bury, N.R.; Walker, P.A.; Glover, C.N. Nutritive metal uptake in teleost fish. *J. Exp. Biol.* **2003**, *206*, 11–23. [CrossRef] [PubMed]
2. Hambidge, K.M.; Krebs, N.F. Zinc deficiency: A special challenge. *J. Nutr.* **2007**, *137*, 1101–1105. [CrossRef] [PubMed]
3. Qu, R.; Feng, M.; Wang, X.; Qin, L.; Wang, C.; Wang, Z.; Wang, L. Metal accumulation and oxidative stress biomarkers in liver of freshwater fish Carassius auratus following in vivo exposure to waterborne zinc under different pH values. *Aquat. Toxicol.* **2014**, *150*, 9–16. [CrossRef] [PubMed]
4. Ranasinghe, P.; Wathurapatha, W.S.; Ishara, M.H.; Jayawardana, R.; Galappatthy, P.; Katulanda, P.; Constantine, G.R. Ef-fects of zinc supplementation on serum lipids: A systematic review and meta-analysis. *Nutr. Metab.* **2015**, *12*, 26. [CrossRef]
5. Kang, X.; Zhong, W.; Liu, J.; Song, Z.; McClain, C.J.; Kang, Y.J.; Zhou, Z. Zinc supplementation reverses alcohol-induced steatosis in mice through reactivating hepatocyte nuclear factor-4alpha and peroxisome proliferator-activated receptor-alpha. *Hepatology* **2009**, *50*, 1241–1250. [CrossRef]
6. Zhang, J.J.; Hao, J.J.; Zhang, Y.R.; Wang, Y.L.; Li, M.Y.; Miao, H.L.; Zou, X.J.; Liang, B. Zinc mediates the SREBP-SCD axis to regulate lipid metabolism in Caenorhabditis elegans. *J. Lipid Res.* **2017**, *58*, 1845–1854. [CrossRef]
7. Wu, K.; Huang, C.; Shi, X.; Chen, F.; Xu, Y.H.; Pan, Y.X.; Luo, Z.; Liu, X. Role and mechanism of the AMPK pathway in waterborne Zn exposure influencing the hepatic energy metabolism of Synechogobius hasta. *Sci. Rep.* **2016**, *6*, 1–13. [CrossRef]
8. Wei, C.C.; Luo, Z.; Hogstrand, C.; Xu, Y.H.; Wu, L.X.; Chen, G.H.; Pan, Y.X.; Song, Y.F. Zinc reduces hepatic lipid deposition and activates lipophagy via Zn2+/MTF-1/PPARα and Ca2+/CaMKKβ/AMPK pathways. *FASEB J.* **2018**, *32*, 6666–6680. [CrossRef]
9. Wu, K.; Luo, Z.; Hogstrand, C.; Chen, G.H.; Wei, C.C.; Li, D.D. Zn stimulates the phospholipids biosynthesis via the pathways of oxidative and endoplasmic reticulum stress in the intestine of freshwater teleost yellow catfish. *Environ. Sci. Technol.* **2018**, *52*, 9206–9214. [CrossRef]

10. Han, S.L.; Qian, Y.C.; Limbu, S.M.; Wang, J.; Chen, L.Q.; Zhang, M.L.; Du, Z.Y. Lipolysis and lipophagy play individual and interactive roles in regulating triacylglycerol and cholesterol homeostasis and mitochondrial form in zebrafish. *BBA-Mol. Cell Biol. L.* **2021**, *1866*, 158988. [CrossRef]

11. Zou, A.; Magee, N.; Deng, F.; Lehn, S.; Zhong, C.; Zhang, Y. Hepatocyte nuclear receptor SHP suppresses inflammation and fibrosis in a mouse model of nonalcoholic steatohepatitis. *J. Biol. Chem.* **2018**, *293*, 8656–8671. [CrossRef] [PubMed]

12. Wu, K.; Zhao, T.; Hogstrand, C.; Xu, Y.C.; Ling, S.C.; Chen, G.H.; Luo, Z. FXR-mediated inhibition of autophagy contributes to FA-induced TG accumulation and accordingly reduces FA-induced lipotoxicity. *Cell Commun. Signal.* **2020**, *18*, 1–16. [CrossRef]

13. Zhang, Y.; Hagedorn, C.H.; Wang, L. Role of nuclear receptor SHP in metabolism and cancer. *BBA-Mol. Basis Dis.* **2011**, *1812*, 893–908. [CrossRef] [PubMed]

14. Chen, S.W.; Lv, W.H.; Wu, K.; Chen, G.H.; Chen, F.; Song, C.C.; Luo, Z. Dietary nano-ZnO is absorbed via endocytosis and ZIP pathways, upregulates lipogenesis, and induces lipotoxicity in the intestine of yellow catfish. *Int. J. Mol. Sci.* **2021**, *22*, 12047. [CrossRef] [PubMed]

15. Roy, A.L.; Singer, D.S. Core promoters in transcription: Old problem, new insights. *Trends Biochem. Sci.* **2015**, *40*, 165–171. [CrossRef] [PubMed]

16. Basehoar, A.D.; Zanton, S.J.; Pugh, B.F. Identification and distinct regulation of yeast TATA box-containing genes. *Cell* **2004**, *116*, 699–709. [CrossRef]

17. Smale, S.T.; Kadonaga, J.T. The RNA polymerase II core promoter. *Annu. Rev. Biochem.* **2003**, *72*, 449–479. [CrossRef]

18. Wu, C.; Sun, M.; Liu, L.; Zhou, G.W. The function of the protein tyrosine phosphatase SHP-1 in cancer. *Gene* **2003**, *306*, 1–12. [CrossRef]

19. Kim, H.J.; Kim, J.Y.; Kim, J.Y.; Park, S.K.; Seo, J.H.; Kim, J.B.; Choi, H.S. Differential regulation of human and mouse orphan nuclear receptor small heterodimer partner promoter by sterol regulatory element binding protein-1. *J. Biol. Chem.* **2004**, *279*, 28122–28131. [CrossRef]

20. Kassam, A.; Capone, J.P.; Rachubinski, R.A. The short heterodimer partner receptor differentially modulates peroxisome proliferator-activated receptor alphamediated transcription from the peroxisome proliferator-response elements of the genes encoding the peroxisomal beta-oxidation enzymes acyl-CoA oxidase and hydratase-dehydrogenase. *Mol. Cell Endocrinol.* **2001**, *176*, 49–56.

21. Frank, C.; Makkonen, H.; Dunlop, T.W.; Matilainen, M.; Vaisanen, S.; Carlberg, C. Identification of pregnane X receptor binding sites in the regulatory regions of genes involved in bile acid homeostasis. *J. Mol. Biol.* **2005**, *346*, 505–519. [CrossRef] [PubMed]

22. Karagianni, P.; Talianidis, I. Transcription factor networks regulating hepatic fatty acid metabolism. *BBA-Mol. Cell Biol. L.* **2015**, *1851*, 2–8. [CrossRef] [PubMed]

23. Norouzi, S.; Adulcikas, J.; Sohal, S.S.; Myers, S. Zinc stimulates glucose oxidation and glycemic control by modulating the insulin signaling pathway in human and mouse skeletal muscle cell lines. *PLoS ONE* **2018**, *13*, e0191727. [CrossRef] [PubMed]

24. Hoeke, M.O.; Heegsma, J.; Hoekstra, M.; Moshage, H.; Faber, K.N. Human FXR regulates SHP expression through direct binding to an LRH-1 binding site, independent of an IR-1 and LRH-1. *PLoS ONE* **2014**, *9*, e88011. [CrossRef]

25. Huang, X.F.; Zhao, W.Y.; Huang, W.D. FXR and liver carcinogenesis. *Acta Pharmacol. Sin.* **2015**, *36*, 37–43. [CrossRef] [PubMed]

26. Lee, Y.S.; Chanda, D.; Sim, J.; Park, Y.Y.; Choi, H.S. Structure and function of the atypical orphan nuclear receptor small heterodimer partner. *Int. Rev. Cytol.* **2007**, *261*, 117–158. [PubMed]

27. Watanabe, M.; Houten, S.M.; Wang, L.; Moschetta, A.; Mangelsdorf, D.J.; Heyman, R.A.; Auwerx, J. Bile acids lower tri-glyceride levels via a pathway involving FXR, SHP, and SREBP-1c. *J. Clin. Investig.* **2004**, *113*, 1408–1418. [CrossRef]

28. Primers, P. High-efficiency thermal asymmetric interlaced PCR for amplification of unknown flanking sequences. *Biotechniques* **2007**, *43*, 649–656.

29. Wu, K.; Tan, X.Y.; Xu, Y.H.; Chen, G.H.; Zhuo, M.Q. Functional analysis of promoters of genes in lipid metabolism and their transcriptional response to STAT3 under leptin signals. *Genes* **2018**, *9*, 334. [CrossRef]

30. Chen, S.W.; Wu, K.; Lv, W.H.; Chen, F.; Song, C.C.; Luo, Z. Functional analysis of two zinc (Zn) transporters (ZIP3 and ZIP8) promoters and their distinct response to MTF1 and RREB1 in the regulation of Zn metabolism. *Int. J. Mol. Sci.* **2020**, *21*, 6135. [CrossRef]

31. Wu, K.; Chen, G.H.; Hogstrand, C.; Ling, S.C.; Wu, L.X.; Luo, Z. Methionine-chelated Zn promotes anabolism by integrating mTOR signal and autophagy pathway in juvenile yellow catfish. *J. Trace Elem. Med. Bio.* **2021**, *65*, 126732. [CrossRef] [PubMed]